Analysis of the Structure of Dendrimers in Solution by Small-Angle Neutron Scattering Including Contrast Variation

D. Pötschke and M. Ballauff*

Polymer-Institut, Universität Karlsruhe, Kaiserstrasse 12, 76128 Karlsruhe, Germany

P. Lindner

Institut Laue-Langevin, BP 156X, 38042 Grenoble, France

M. Fischer and F. Vögtle

Kekulé-Institut für Organische Chemie und Biochemie, Gerhard-Domagk-Str. 1, 53121 Bonn, Germany

Received December 29, 1998; Revised Manuscript Received April 2, 1999

ABSTRACT: The analysis of a dendrimer of fifth generation by small-angle neutron scattering (SANS) in solution is presented. The contrast of the solute toward the solvent dimethylacetamide (DMA) is changed systematically by measurements of the dendrimer in mixtures of deuterated with protonated DMA. Additional SANS measurements at highest contrast and varying dendrimer concentrations allowed to determine the structure factor of the dendrimers in solution. SANS intensities measured at different contrast are shown to yield the contrast $\bar{\rho} - \rho_m$ where $\bar{\rho}$ is the average scattering length density of the dissolved dendrimer and ρ_m is the scattering length density of the solvent. This allows to determine the molecular weight of the dendrimer in an unambiguous fashion. The comparison of the measured and the calculated molecular weight demonstrates that the dendritic structure under consideration here is not fully perfect. The analysis of the radial structure of the dendrimer rests on the decomposition of the measured intensities into terms depending on powers of the contrast $\bar{\rho} - \rho_m$. The leading term which scales with the square of the contrast leads to the determination of the scattering intensity referring to infinite contrast. This allows to elucidate the radial scattering length density in an unambiguous manner. The analysis demonstrates that the present dendrimer, composed of flexible units, has a compact structure where the density has its maximum at the center of the molecule. This is in accord with recent theoretical deductions.

Introduction

Dendrimers are synthetic macromolecules with defined architecture which are synthesized by iterative controlled reaction steps.[1−3] Starting from a trifunctional monomer (generation 0), subsequent generations are connected to this initial core which results in a treelike structure. Since the mass of the molecule increases exponentially with the number of generations and grows more rapidly than the available volume, the structure is expected to saturate at a given generation number. In this respect dendrimers represent interesting intermediates between linear polymers and colloid particles: At low generation number the structure will be akin to the one of star polymers having a great number of available conformations. At high generation number, however, a rather densely packed radial structure will result with less internal degrees of freedom. At this stage, significant back-folding must result.

The first theoretical treatment of the structure of dendrimers has been given by de Gennes and Hervet.[4] These authors derived a density profile that has a minimum at the center of the starburst and increased monotonically to the outer edge. In contrast to this, Lescanec and Muthukumar found the density to exhibit its maximum at the center of the molecule.[5] Manfield and Klushin performed a series of Monte Carlo Studies of dendrimers up to the ninth generation.[6] Their study corroborated qualitatively the results presented by Lescanec and Muthukumar. More recently, Murat and Grest presented a molecular dynamics study that included the effect of solvent quality on the internal structure of dendrimers.[7] A further study of the structure of dendrimers employing molecular dynamics was presented by Cavallo and Fraternali.[8] Radial atom densities as a function of the distance from the center of mass have been derived and discussed by these authors. The equilibrium structure of dendrimers was recently the subject of a comprehensive study by Boris and Rubinstein.[9] These workers developed a Flory model of the starburst structure, the results of which were subsequently corroborated by a self-consistent mean-field model. The theory of Boris and Rubinstein allows to understand the basic factors controlling the size of dendritic structures as a function of solvent power. These authors also made detailed prediction regarding the scattering function of dendrimers and showed that small-angle scattering is capable of distinguishing between different models of the radial structure. Very recently, Welch and Muthukumar demonstrated the strong influence of charges within the dendrimer which may lead to a transition between a dense core and a dense shell structure.[10]

From these theoretical studies is seems to be well-established that uncharged dendritic structures should have the maximum of the density at the center of the molecule. On the other hand, Uppuluri et al. proposed a structure with a dense shell in order to explain rheological data.[11] Thus, the internal structure of dendrimers seems to be still a matter of debate despite a decade of intense research.

* To whom all correspondence should be addressed.

10.1021/ma982027x CCC: $18.00 © 1999 American Chemical Society
Published on Web 05/20/1999

Compared to these detailed theoretical studies, the number of experimental investigations devoted to the structure of dendrimers is scarce.[12−16] A study by small-angle X-ray scattering (SAXS) conducted by Prosa et al.[14] demonstrated clearly the transition of a polymer-like scattering behavior to the scattering pattern of a colloidal structure with increasing number of generations: For low generations a virtually structureless scattering curve resulted whereas the dendrimer of generation 10 exhibited two side maxima in the measured SAXS intensity $I(q)$ as a function of the magnitude of the scattering vector q [$q = (4\pi/\lambda)\sin(\theta/2)$, where λ is the wavelength of radiation and θ the scattering angle). These side maxima are indicative of a rather dense spherical structure[17] expected for dendritic structures of this generation. A study using small-angle neutron scattering (SANS) by Scherrenberg et al.[15] showed the similar trend. Here a distinct maximum showed up in Kratky plots $I(q)q^2$ vs q with increasing number of generation. This feature is in qualitative accord with the findings of Boris and Rubinstein (see Figure 11 of ref 9).

All previous SANS and SAXS investigations were conducted at a given contrast of the dendrimer toward the solvent used in the respective studies. Here a number of problems arise that render a direct comparison of theory and experiment a difficult task: SANS and SAXS are sensitive not only to this distribution but also to inhomogeneities deriving from the different scattering lengths[18] of the atoms constituting the dendritic structure. Therefore, different groups within the dendrimer will contribute differently to the measured scattering intensity $I(q)$. The presence of groups inside the dendritic structure that have a different scattering length density is followed by an additional contribution to the measured scattering intensity. This part of $I(q)$ must be removed prior to comparison with theory. Moreover, the constitutive units of the dendritic structure can no longer be regarded as point scatterers but as objects of finite size having an internal density distribution. This fact must be kept in mind when comparing the scattering function measured at high q values to theoretical data.

Another serious problem of SANS investigations is given by the incoherent contribution to the intensity due to the great number of hydrogen atoms in the structure.[18] This contribution does not depend on contrast and may constitute a nonnegligible part of the measured intensity at high q values. This is a problem of particular importance when measuring the scattering function of small objects in solution.

In addition to this, dendrimers are structures that have certainly larger dimensions than the surrounding solvent molecules, but the difference is only about 1−2 orders of magnitude. Treating the solvent as an incompressible continuum may therefore lead to errors,[19] because fluctuations of the density of the solvent around the dendrimer may lead to concomitant fluctuations of the contrast which must be addressed properly.

Most of these contributions are small or negligible if polymeric objects comprising a great number of scattering units are investigated by SANS. The coherent part of $I(q)$ scales with n^2 where n is the number of monomer units. The incoherent part scales only with n and is negligible for large n. In case of small objects as for example dendrimers, however, possible incoherent contributions must be removed to allow for a meaningful structural study of dendritic molecules.

SANS offers the unique possibility to address these problems by change of the contrast between solute and solvent through use of mixtures of deuterated and protonated solvents.[18] The method termed contrast variation allows to distinguish between the scattering signal due to the outer shape of the object and the scattering signal due to the variation of the density inside the object.[17,18,20−23] Moreover, contributions that are independent of contrast as for example the incoherent contribution may be determined and subtracted from the measured intensity.

Here we present the results of a comprehensive SANS investigation of a dendritic structure of fifth generation (see Figure 1). The synthesis and characterization of a similar dendrimer of fourth generation has been given recently.[24] Here diphenyl ether end groups have been attached to a dendrimer of fifth generation. The structure is akin to the dendrimer simulated in ref 8. The dendrimer exhibits good solubility in dimethylacetamide (DMA). In the course of the present study the contrast of the solute toward the solvent has been changed by use of appropriate mixtures of deuterated DMA with protonated DMA. The main goal of the present investigation is the determination of the radial density profile of the dendrimer.

Theory

We consider a system of monodisperse objects with number density N oriented at random. The scattering intensity $I(q)$ as a function of q, the magnitude of the scattering vector, may be rendered as[17,18]

$$I(q) = NI_0(q)\,S(q) + NI_{\mathrm{incoh}} \tag{1}$$

where $I_0(q)$ is the scattering intensity of a single particle at infinite dilution and $S(q)$ denotes the structure factor that takes into account the interparticular interferences.[17,18] The influence of $S(q)$ will make itself felt even at low concentration and must be removed through proper extrapolation to vanishing concentration (see below). In addition to these terms which are determined by the spatial structure of the dissolved molecule, $I(q)$ may also contain an incoherent part I_{incoh} which is due to the reasons discussed above. I_{incoh} may become a nonnegligible contribution to $I(q)$ at high scattering angles.

In general, $I_0(q)$ referring to particles immersed in a solvent of scattering length density ρ_m can be calculated by use of the Debye equation[17]

$$I_0(q) = \int\int [\rho(\vec{r}_1) - \rho_m][\rho(\vec{r}_2) - \rho_m]\frac{(\sin(q|\vec{r}_1 - \vec{r}_2|)}{q|\vec{r}_1 - \vec{r}_2|}\,\mathrm{d}\vec{r}_1\,\mathrm{d}\vec{r}_2 \tag{2}$$

where $\rho(\vec{r})$ is the scattering length density at point $\vec{r}$. Following refs 17 and 20, this quantity is rendered as the product of a shape function $T(\vec{r})$ and the local scattering length density $\rho_p(\vec{r})$ inside the object:

$$\rho(\vec{r}) = T(\vec{r})\,\rho_p(\vec{r}) + \rho_m[1 - T(\vec{r})] \tag{3}$$

The local scattering length density $\rho_p(\vec{r})$ refers to the hypothetical structure of the object in vacuo. All information to be obtained from an analysis of the crystal structure is embodied in $\rho_p(\vec{r})$. In contrast to this, the

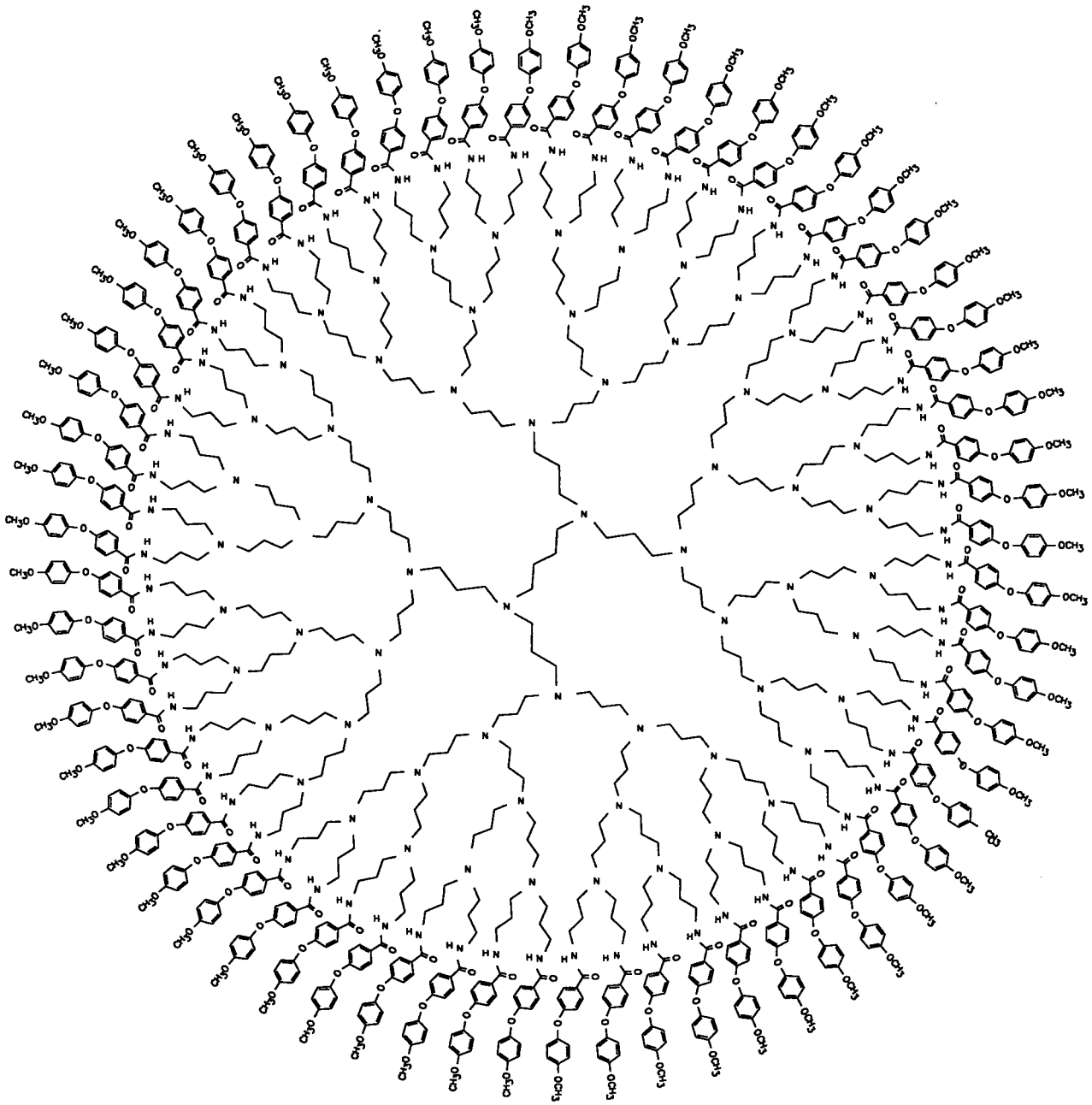

Figure 1. Chemical structure of the dendrimer of fifth generation.

shape function $T(\vec{r})$ describes the spatial structure assumed by the object in solution, i.e., the shape of the cavity in which the solvent has been replaced by the object. When discussing these quantities and functions, it must also be kept in mind that the dendritic object under consideration here has a diameter of a few nanometers only. The monomeric units building up the structure have a size hardly exceeding that of the solvent. It is therefore evident that the penetration of the solvent into the dendritic structure may depend on the solvent used in the scattering experiment. The shape function $T(\vec{r})$ is therefore governed not only by the structure of the solute but also by the ability of the solvent to penetrate into the structure. To account for this effect and for the finite resolution of the scattering experiment, $T(\vec{r})$ is allowed to vary continuously between 0 and 1 (cf. refs 17 and 20).

Furthermore, the shape function derived from experimental data describes the statistical-mechanical average of a centrosymmetric but fluctuating object. By virtue of this averaging, the shape function of the centrosymmetric dendrimer considered here will be a function of the distance r of the center of gravity only. Therefore, $T(r)$ corresponds to the average over $T(\vec{r})$ of all possible conformers and orientations and gives the probability of finding a segment at a distance r; i.e., $4\pi T(r)r^2\,\mathrm{d}r$ is the volume of all segments located in a spherical shell at distance r. It is obvious from this that the shape function describing the conformation of such a statistically fluctuating object must be a function that varies continuously between 0 and 1.

From the above definition of $T(\vec{r})$ it follows directly that the partial volume V_p of the particles is given by

$$V_p = \int T(\vec{r})\,\mathrm{d}\vec{r} \tag{4}$$

Hence, V_p is the volume of the particular solvent replaced by the solute. The volume fraction ϕ of the

solute is therefore given by $\phi = NV_p$. The average scattering length density $\bar{\rho}$ in this system follows as

$$\bar{\rho} = \frac{1}{V_p}\int T(\vec{r})\,\rho_p(\vec{r})\,\mathrm{d}\vec{r} \tag{5}$$

and the difference $\bar{\rho} - \rho_m$ is the contrast of the object toward the solvent. The average scattering length density refers therefore to the volume V_p occupied by the particles in a given solvent and not to the volume occupied in the dry state, i.e., in vacuo.

Given these basic prerequisites and definitions, the excess scattering length density $g(\vec{r},\rho_m)$ may be split into a part depending on the contrast $\bar{\rho} - \rho_m$ and into a function $\Delta\rho(\vec{r})$ independent of contrast:[20]

$$g(\vec{r},\rho_m) = \rho(\vec{r}) - \rho_m = T(\vec{r})[\bar{\rho} - \rho_m] + T(\vec{r})\,\Delta\rho(\vec{r}) \tag{6}$$

Equation 6 defines the function $T(\vec{r})\Delta\rho(\vec{r})$ which describes the deviations of the scattering length density from its mean value inside the object. From eqs 5 and 6 it is evident that

$$\int T(\vec{r})\,\Delta\rho(\vec{r})\,\mathrm{d}\vec{r} = 0 \tag{7}$$

Introduction of eq 6 into eq 2 leads to the splitting of the scattering intensity $I_0(q)$ into three parts:

$$I_0(q) = [\bar{\rho} - \rho_m]^2 I_S(q) + 2[\bar{\rho} - \rho_m]I_{SI}(q) + I_I(q) \tag{8}$$

where

$$I_S(q) = \int\int T(\vec{r}_1)\,T(\vec{r}_2)\frac{\sin(q|\vec{r}_1 - \vec{r}_2|)}{q|\vec{r}_1 - \vec{r}_2|}\,\mathrm{d}\vec{r}_1\,\mathrm{d}\vec{r}_2 \tag{9}$$

and

$$I_{SI}(q) = \int\int T(\vec{r}_1)\,T(\vec{r}_2)\,\Delta\rho(\vec{r}_2)\frac{\sin(q|\vec{r}_1 - \vec{r}_2|)}{q|\vec{r}_1 - \vec{r}_2|}\,\mathrm{d}\vec{r}_1\,\mathrm{d}\vec{r}_2 \tag{10}$$

and

$$I_I(q) = \int\int T(\vec{r}_1)\,\Delta\rho(\vec{r}_1)\,T(\vec{r}_2) \times \Delta\rho(\vec{r}_2)\frac{\sin(q|\vec{r}_1 - \vec{r}_2|)}{q|\vec{r}_1 - \vec{r}_2|}\,\mathrm{d}\vec{r}_1\,\mathrm{d}\vec{r}_2 \tag{11}$$

Here $I_S(q)$ is the scattering contribution referring to an object the shape of which is defined by $T(\vec{r})$. $I_I(q)$ is related to inhomogeneities that result from the fact that not all atoms and groups constituting the dendritic structure have the same scattering length.

The three different contributions defined in eqs 8−11 are related to the structure of the object and constitute coherent parts of $I(q)$. As mentioned in the Introduction, a further contribution to the measured intensity may arise from the density fluctuations of the solvent. On one hand, these fluctuations of the solvent density lead to the scattering background which is removed as usual during the evaluation of the data (see Experimental Section). On the other hand, fluctuations of the solvent density must necessarily be followed by small fluctuations of the contrast $\bar{\rho} - \rho_m$. This is directly evident when considering a homogeneous object embedded in a solvent that exactly matches its scattering length density $\bar{\rho}$. No scattering can be observed in this case if the solvent is completely homogeneous. If ρ_m fluctuates, a small but finite scattering intensity arises which is uncorrelated to the structure of the dissolved object. The magnitude of this term is difficult to estimate, however. It is important to note that this term has no cross-term with $I_S(q)$. This again is due to the fact that the fluctuations of solvent density are uncorrelated to the equilibrium structure of the dendrimer. In the following this term will be treated as another contribution to I_{incoh}.

For $q \to 0$, eq 8 in conjunction with eq 7 leads to the conclusion that

$$NI_0(0) = N[\bar{\rho} - \rho_m]^2 V_p^2 = \phi[\bar{\rho} - \rho_m]^2 V_p \tag{12}$$

Hence, the forward scattering of the solute is solely determined by $I_S(q)$ if I_{incoh} constitutes only a negligible part at small q values. In this case plots of $I_0(0)^{1/2}$ vs ρ_m can be used to determine the average scattering length density. If I_{incoh} is not negligible against $I_S(0)$, however, plots according to eq 12 may lead to erroneous data for the average scattering length density. At small q the measured intensity $I(q)$ must exhibit its minimal value if $\rho_m = \bar{\rho}$, i.e., if the scattering length density of the solvent matches the one of the object. For $q \to 0$ and $\rho_m = \bar{\rho}$ the extrapolated intensity $I(0)$ is solely given by the q-independent term I_{incoh}. Therefore, plots of $I_0(q)$ vs ρ_m for small q may serve for the determination of $\bar{\rho}$ as well.

At small q the scattering intensity normalized to the volume fraction of the solute may be approximated by Guinier's law[15,16]

$$\frac{I(q)}{\phi} \cong V_p(\bar{\rho} - \rho_m)^2 \exp\left(-\frac{R_g^2}{3}q^2\right) \tag{13}$$

where R_g denotes the radius of gyration. Its dependence on contrast $\bar{\rho} - \rho_m$ is given by[22,23]

$$R_g^2 = R_{g,\infty}^2 + \frac{\alpha\bar{\rho}}{\bar{\rho} - \rho_m} - \beta(\bar{\rho} - \rho_m)^{-2} \tag{14}$$

Here $R_{g,\infty}$ denotes the radius of gyration at infinite contrast, i.e., of the shape function, whereas the coefficient α is given by

$$\alpha = (\bar{\rho}V_p)^{-1}\int_0^\infty T(\vec{r})\,\Delta\rho(\vec{r})r^2\,\mathrm{d}V \tag{15}$$

The quantity α therefore may be regarded as the radius of gyration of the internal variation of scattering length density $T(\vec{r})\Delta\rho(\vec{r})$. The coefficient β is the average square distance between the centers of gravity of the distributions $T(\vec{r})$ and $T(\vec{r})\Delta\rho(\vec{r})$.[17,23] It vanishes for a centrosymmetric object. Hence, for the average shape function to be determined here, β is expected to be zero. Equation 14 also demonstrates that only $I_S(q)$ and $I_I(q)$ will contribute to $I_0(q)$ in the Guinier regime; the cross term $I_{SI}(q)$ has only contributions of $O(q^4)$.

Having determined $\bar{\rho}$, the measured scattering intensity $I(q)$ can be decomposed according to eq 8. This leads to the unambiguous determination of $I_S(q)$ which is related to the shape function $T(r)$ through eq 9. $I_S(q)$ refers to the scattering intensity measured at infinite contrast where all other terms in eq 8 may be neglected. Hence, contrast variation allows to extract the contribution that contains the structural information through

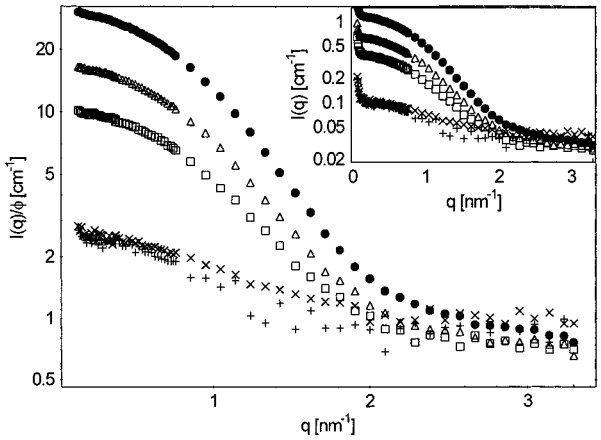

Figure 2. Scattering intensity (0.14 $nm^{-1} \leq q \leq 3.3\ nm^{-1}$) of the dissolved dendrimer normalized volume fraction ϕ measured at different contrast. The contrast has been adjusted by appropriate mixtures of DMA-D_9 and DMA-H_9. The inset shows the raw data in the entire q range. The numbers in parentheses give the contrast $\bar{\rho} - \rho_m/10^{10}\ cm^{-2}$. ●, 100% DMA-$D_9$ (−4.55); △, 80/20 DMA-D_9/DMA-H_9 (−3.42); □, 60/40 DMA-D_9/DMA-H_9 (−2.53); ×, 40/60 DMA-D_9/DMA-H_9 (−1.14); +, DMA-H_9 (+1.18).

Fourier transformation of $T(r)$. The other terms defy direct interpretation since $I_I(q)$ cannot be separated from I_{incoh}.

Experimental Section

Protonated DMA (DMA-H_9, Fluka, analytical grade) and deuterated DMA (DMA-D_9, Deutero GmbH, 98% deuteration) were used as received. The dendrimer shown in Figure 1 was synthesized as described recently.[24]

All SANS measurements have been conducted using the D11 instrument of the Institut Laue-Langevin in Grenoble using a wavelength of 0.6 nm. The range of scattering vectors was 0.07−3.3 nm^{-1} using three different positions of the detector.[25] The dendrimer was dissolved in DMA-D_9 in concentrations ranging from 9.4 to 46.6 g/L to explore the influence of finite concentrations. Contrast variation was done by using mixtures of DMA-H_9 and DMA-D_9; the concentration of the dendrimer was 45 g/L in these solutions. Absolute intensities at a detector distance of 5 m were obtained by normalizing the intensity scale by using the strong incoherent scattering of water as a standard. The absolute scattering cross section of H_2O was calculated for the wavelength of 0.6 nm using the relation of Ragnetti et al.[26] Data deriving from measurements taken at different positions of the detector were normalized by using an appropriate factor determined from measurements of a Teflon probe.

The contribution $I(q)$ of the dissolved dendrimer was separated from the contribution of the solvent $I_1(q)$ by[21]

$$I(q) = I_{solution}(q) - (1 - \phi)I_1(q) \qquad (16)$$

Densities of the solutions were measured using a DMA-60 densitometer (Paar, Graz, Austria). The partial molar volume v_2 of the dendrimer resulted to 0.84 cm^3/g. Volume fractions in the dilute regime have been obtained from the weight concentrations c through $\phi = cv_2$.

Results and Discussion

As mentioned in the Introduction, the present analysis rests on measurements of the dendrimer at different contrast. Figure 2 displays the scattering intensities obtained by application of eq 16 to the data measured in four different solvent mixtures. For all contrast statistically sound data could be obtained up to at least $q = 2.5\ nm^{-1}$; beyond this point the data taken at lowest contrast are less secure and will be omitted in the analysis by contrast variation.

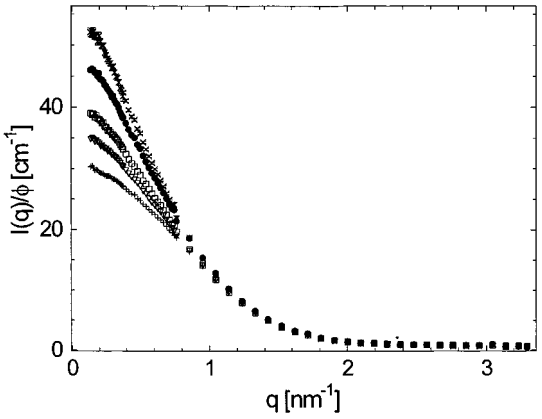

Figure 3. Influence of $S(q)$ on the scattering intensity $I(q)$ measured at highest contrast (in DMA-D_9): Scattering intensity normalized to volume fraction vs magnitude of scattering vector q. The respective volume fractions ϕ are (+) 0.039, (▽) 0.026, (□) 0.016, (●) 0.008, and (×) extrapolated to $\phi = 0$ according to eq 17 (cf. Figure 4).

There is some indication of a weak association which leads to an upturn of the scattering intensities at lowest scattering vectors q. This is demonstrated in the inset of Figure 2, which displays the measured scattering intensities over the entire q range. The upturn visible only at the first points can be explained by the presence of a few aggregates which could not be avoided despite careful preparation of the solutions. A possible reason for this weak attractive interaction between the dendrimers may be located in the presence of some imperfect structures (see below). The signal of these aggregates is restricted to the first few points and can be omitted in the subsequent analysis of the data. Hence, in what is to follow only data between 0.14 and 3.3 nm^{-1} have been taken into account.

To determine the influence of concentration expressed through the structure factor $S(q)$ (cf. eq 1), measurements have been performed at different concentrations (9.4−46.6 g/L) at the highest possible contrast in DMA-D_9. Figure 3 displays the intensities normalized to the volume fraction ϕ.

To discuss the influence of concentration on $I(q)$ in the dilute regime, it is permissible to treat the dilute solution of dendrimers in terms of an effective diameter d which is the minimum distance to which two spheres may approach each other (cf. the discussion of this point in ref 21). For the small concentrations under consideration here, binary interactions between the spheres will prevail. Therefore, $S(q)$ may be approximated as[21]

$$\frac{1}{S(q)} = 1 + 2B_{app}\phi + O(\phi^2) \qquad (17)$$

with the apparent virial coefficient B_{app} given by[21]

$$B_{app} = 4\frac{(4\pi/3)d^3}{V_p}\left(1 - \frac{1}{10}d^2q^2 + ...\right) \qquad (18)$$

This suggests the extrapolation of $I_0(q)$ by plots of $\phi/I(q)$ vs ϕ for given scattering angles. The intercept yields the normalized reciprocal scattering intensity at $\phi = 0$. The slope of these lines is expected to decrease with q. Figure 4 displays the extrapolation to vanishing concentration. Good linearity is observed for all q values under

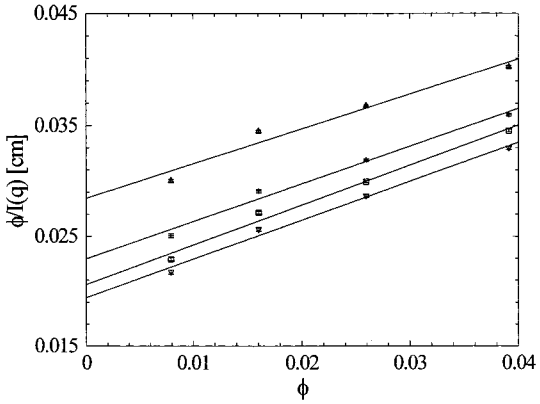

Figure 4. Extrapolation of the scattering intensity to vanishing volume fraction using eq 17. $\phi/I(q)$ vs ϕ for four different q values: △, $q = 0.5$ nm^{-1}; +, $q = 0.34$ nm^{-1}; □, $q = 0.24$ nm^{-1}; ▽, $q = 0.14$ nm^{-1}.

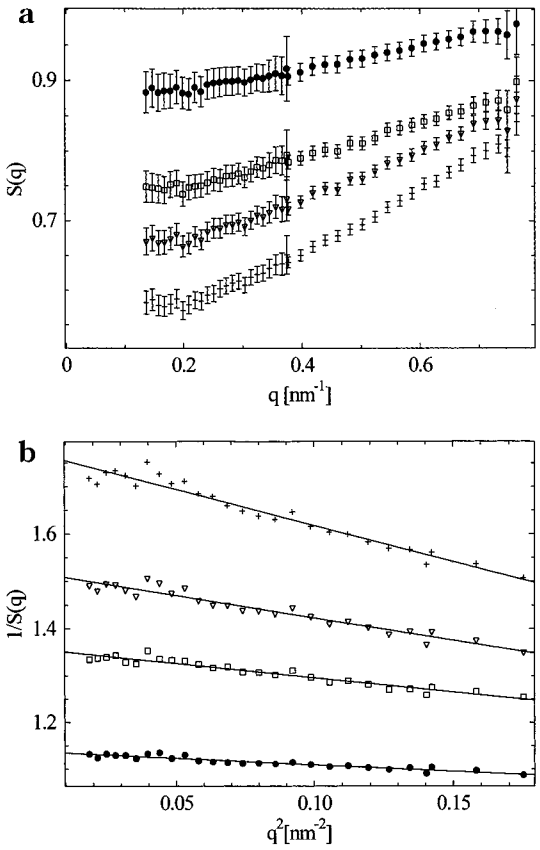

Figure 5. Dependence of the structure factor on volume fraction and q. (a) $S(q)$ as a function of q for four different volume fractions: +, 0.039; ▽, 0.026; □, 0.016; ●, 0.008. (b) Dependence of $S(q)$ on q according to eqs 17 and 18. $1/S(q)$ vs q^2 for four volume fractions: +, 0.039; ▽, 0.026; □, $\phi = 0.016$; ●, $\phi = 0.008$.

consideration here which corroborates the analysis according to eqs 17 and 18. It also becomes obvious from Figure 4 that in the present q range none of the used concentrations are small enough to render the influence of $S(q)$ negligible. The uppermost curve in Figure 3 displays the resulting intensity data $I(q)/\phi$ which have been extrapolated to vanishing volume fraction.

The data of $I(q)/\phi$ at $\phi = 0$ thus obtained may now serve for the evaluation of the structure factor $S(q)$ according to eq 1. Figure 5a displays $S(q)$ thus obtained. Since the concentrations are much smaller than in case of the study by Ramzi et al.,[16] no distinct maximum of

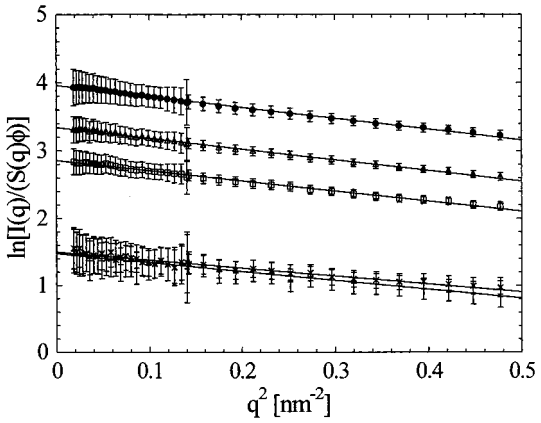

Figure 6. Guinier plots of the scattering intensities measured at different contrast. All data have been extrapolated to vanishing concentration as described in ref 21. The curves refer to different contrasts as adjusted by using mixtures of deuterated DMA (DMA-H_9) and protonated DMA (DMA-H_9) indicated by the weight ratio of DMA-D_9 to DMA-H_9. The numbers in parentheses give the contrast $\bar{\rho} - \rho_m/10^{10}$ cm^{-2}. ●, 100% DMA-D_9 (−4.55); △, 80/20 DMA-D_9/DMA-H_9 (−3.42); □, 60/40 DMA-D_9/DMA-H_9 (−2.53); ×, 40/60 DMA-D_9/DMA-H_9 (−1.14); +, DMA-H_9 (+1.18).

$S(q)$ as a function of q can be seen. Figure 5b demonstrates that eq 17 together with eq 18 provides a reasonable fit for the data at low volume fractions and low q values. The evaluation of the slope and the intercept gives an effective diameter of interaction $d =$ 2.5−3 nm. This is slightly lower than is expected from the structural data to be discussed for below which would suggest an effective diameter of 4−5 nm. It must be kept in mind that the determination of d from $S(q)$ is afflicted by an appreciable error which is difficult to assess. Moreover, data at still lower q have demonstrated that there is some weak attraction between the dendrimers (see above the discussion of Figure 2) which will lower d as well.

The above data of $S(q)$ can be used to calculate the scattering intensities $I_0(q)$ obtained at different contrast because $S(q)$ does not depend on contrast. This is due to the fact that we deal here with a practically monodisperse system. For suspensions containing particles of different size and composition, however, the measured structure factor obtained by $I(q)/I_0(q)$ is function of contrast as well.[27] In the present case division of the measured intensity $I(q)$ by $S(q)$ obtained for the respective volume fraction ϕ leads to $I_0(q)$ for a given contrast. Hence, it suffices to measure $S(q)$ for the highest possible contrast, i.e., for the dendrimers dissolved in DMA-D_9. In the following all data have been divided by $S(q)$ to remove the influence of interparticular interferences.

Figure 6 displays Guinier plots of the scattering intensities taken at different contrast. Good linearity is seen at all contrasts in the given q range which gives accurate values of $I(0)/\phi$ and the radius of gyration R_g as a function of contrast. As suggested by eq 12, a plot of the square root of the intercepts vs ρ_m allows to obtain $\bar{\rho}$ and V_p. Figure 7 demonstrates that $(I(0)/\phi)^{1/2}$ is a linear function of ρ_m indeed. The average scattering length density $\bar{\rho} = 1.71 \times 10^{10}$ cm^{-2}, which is in good agreement with the calculated value $\bar{\rho} = 1.68 \times 10^{10}$ cm^{-2}. The volume V_p follows from the slope as $V_p = 26.1$ nm^3.

In addition to this, plots of $I(q)$ vs ρ_m in the region of small angles showed that the minimum of $I(q)$ is located

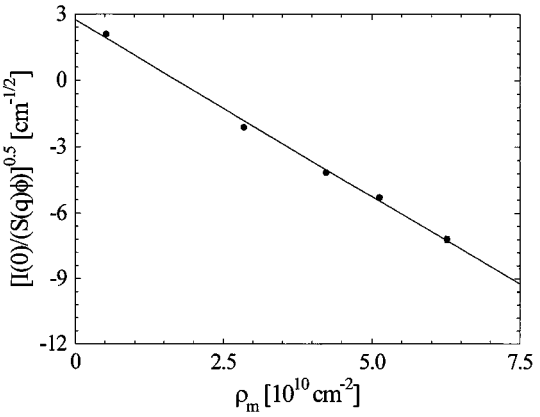

Figure 7. Plot of the square root of the forward scattering intensity $I(0)/(\phi S(q))$ obtained from the Guinier extrapolation eq 13 (see Figure 6) vs the scattering length density of the solvent (mixtures of DMA-H_9 and DMA-D_9). The sign of the square root has been determined by the sign of the respective contrast. The slope gives the volume of the dendrimers V_p = 26.1 nm^3 whereas the intercept yields the average scattering length density $\bar{\rho} = 1.71 \times 10^{10}$ cm^{-2}.

at $\rho_m = 1.69 \times 10^{10}$ cm^{-2}. It is thus obvious that the incoherent part I_{incoh} is a small contribution near $q = 0$, and plots of the square root of the forward scattering $I(0)$ lead to correct values of the contrast. While I_{incoh} is practically negligible at small q, its contribution at high q will turn out to be important as compared to $I_S(q)$ (see below).

The molecular weight resulting from this analysis is given by 18 700 ± 500 g/mol instead of the theoretical value of 21 647 g/mol calculated from the chemical formula. This shows that the dendrimer studied here is not fully perfect.[28] It must be noted that only contrast variation allows to obtain $\bar{\rho}$ and V_p independently. If measurements are only done at one contrast, V_p or the molecular weight of the dendrimers cannot be determined unambiguously. From eq 13 it is obvious that in this case $\bar{\rho}$ cannot be obtained independently but must be calculated from the chemical structure of the particle or molecule. Defects in the structure, however, will affect $\bar{\rho}$ as well and introduce a considerable error into the calculation of the molecular weight. SANS in conjunction with contrast variation, however, yields both $\bar{\rho}$ and V_p. Hence, SANS furnishes valuable information on the overall size of the dendrimers and thereby on possible faults in these structures. In this respect, SANS supplements the information obtained by mass spectrometry.[28]

The experimental value of the average scattering length density $\bar{\rho}$ is the base for analyzing the dependence of R_g on contrast according to eq 14. Figure 8 displays the Stuhrmann plot[17,22] of the R_g. The radius of gyration exhibits a small dependence on contrast. From Figure 8 we obtain $R_{g,\infty} = 2.15$ nm and $\alpha = 0.13$ nm. Within the present limits of error, β is zero as expected for a centrosymmetric distribution. The value of α is too small to be interpreted in terms of structural details. It may also be afflicted by the incoherent contributions discussed above. Its magnitude, however, allows to draw one important conclusion: Given the fact that the dendritic core has a different contrast ($\bar{\rho} \approx 1.73 \times 10^{10}$ cm^{-2}) than the diphenyl ether end groups ($\bar{\rho} \approx 1.83 \times 10^{10}$ cm^{-2}), this finding shows that the dendritic structure under consideration must fluctuate strongly. If the dendrimer would have a distinct core−shell structure with the end groups being always located at

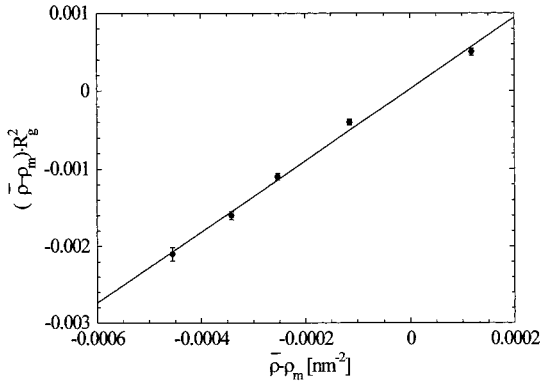

Figure 8. Stuhrmann plot (cf. eq 14) of the radii of gyration obtained from the Guinier plot Figure 6.

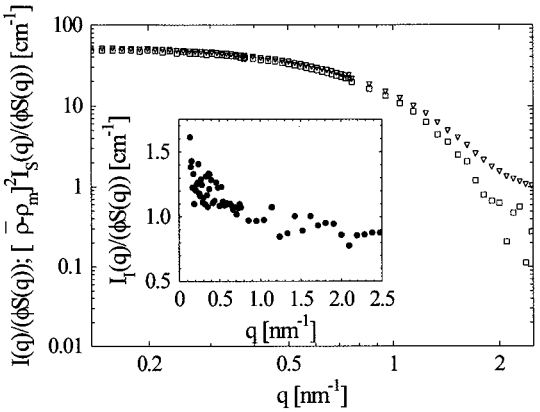

Figure 9. Comparison of the different contributions to the measured scattering intensity $I(q)$ according to eq 8. The triangles give the measured intensity extrapolated to vanishing volume fraction ($I(q)/(S(q)\phi)$). The squares show the contribution $[\bar{\rho} - \rho_M]^2 I_S(q)$, i.e., the part of $I(q)$ that scales with the square of the contrast (cf. eq 8). The inset displays the contribution $I_I(q)$ which is independent of contrast.

the periphery of the molecule, a characteristic change of R_g with contrast would result (cf. the discussion of this point in refs 23 and 29).

With the contrast $\bar{\rho} - \rho_m$ being known, the measured scattering intensity $I(q)$ now may be decomposed into three contributions according to eq 8. As discussed above, the cross term $I_{SI}(q)$ only contributes to $O(q^{-4})$ and is therefore to be omitted in the Guinier range. Its contribution turned out to be marginal at higher q as well. Figure 9 gives both $I_S(q)$ and $I_I(q)$ obtained by this decomposition of $I_0(q)$ together with the data for $I_0(q)$ obtained at highest contrast (triangles). The term $I_I(q)$ shown in the inset presents a small but nonzero contribution to the measured scattering intensity $I(q)$. As discussed in the theoretical section, $I_I(q)$ contains also the sum of the incoherent contributions I_{incoh} and is therefore difficult to interpret. In what is to follow, we therefore discuss only $I_S(q)$, i.e., the leading contribution which scales with the square of the contrast.

$I_S(q)$ may be obtained from the above analysis without difficulty. At small q it practically coincides with $I_0(q)$ derived from measurements at highest contrast. There are marked differences beyond $q = 1$ nm^{-1}, however. Only $I_S(q)$ is related to the spatial structure of the dendrimer and can be compared to theoretical models. Residual contributions from I_{incoh} and $I(q)$ would profoundly disturb this comparison, of course.

The shape function $T(r)$ which presents the main information to be drawn from the present scattering

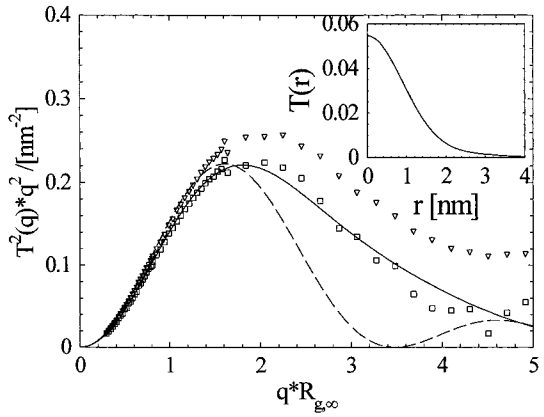

Figure 10. Scattering intensities of the dendrimer in Kratky representation vs magnitude of scattering vector q. The triangles mark the scattering intensities measured at highest contrast (in fully deuterated DMA) normalized to unity at $q = 0$. The squares give $(\bar{\rho} - \rho_m)^2 T^2(q)$. The latter part has been determined according to eq 8 from measurements taken at different contrast using the average scattering length density $\bar{\rho}$. The solid line gives the best fit of the latter term by the expression given by eq 21. The inset displays $T(r)$ obtained from $T(q)$ by Fourier inversion of eq 21. The dashed line gives the scattering intensity of a homogeneous sphere having the radius of gyration $R_{g,\infty}$.

experiments may be obtained by Fourier inversion of $I_S(q)$. This can be achieved as follows: The previous analysis has clearly demonstrated that $I_S(q)$ is the Fourier transform of a centrosymmetric distribution $T(r)$. Therefore, it follows that

$$I_S(q) = T^2(q) \tag{19}$$

where $T(q)$ is given by

$$T(q) = 4\pi \int T(r) \frac{\sin qr}{qr} r^2 \, dr \tag{20}$$

It is obvious that the experimental data are restricted to a given q range. Direct numerical inversion therefore would lead to truncation effects. To circumvent this difficulty, $T(q)$ obtained from $I_S(q)$ by application of eq 19 is fitted by the following empirical expression:

$$T^2(q) = {V_p}^2 \exp[-q^2 {R_{g,\infty}}^2/3] + (aq^2 + bq) \exp(-dq^2) \tag{21}$$

In this expression the first terms ensures the correct rendition of the data in the range where eq 4 is valid. The second term is purely empirical and gives an optimal description of the data at high q values.

To display the difference between $I_S(q)$ and $I_0(q)$ more clearly, Figure 10 gives a Kratky plot of both intensities. For better comparison with theory, the abscissa has been scaled by the radius of gyration $R_{g,\infty}$ referring to infinite contrast. The solid line in Figure 10 refers to a fit of the experimental $T^2(q)$ by eq 21. It demonstrates that the above expression yields a description for the entire range of q values available from experiment. It must be kept in mind, however, that $T^2(q)$ as given by eq 21 presents a continuation to much higher q values which are not available experimentally. The present experimental data extend to $qR_{g,\infty} \leq 5$. In consequence, this q range allows to make firm conclusions about the overall shape of $T(r)$; smaller details in the subnanometer range cannot be resolved by the present set of data.

It is obvious, however, that $I_S(q)$ deviates markedly from the measured intensity at highest contrast when going beyond the Guinier range. It demonstrates that contributions independent of contrast come into play for $qR_{g,\infty} > 2$ and must be subtracted properly.

The inset shows the function $T(r)$ derived from Fourier inversion of the $T(q)$ fitted by the expression eq 21. As expected from recent theoretical treatments,[5,6,9] the function $T(r)$ exhibits its maximum at the center and falls of to zero within ca. 3 nm. As mentioned above when discussing the radius of gyration, there is no distinct core−shell structure, but $T(r)$ decreases smoothly. The entire structure has therefore a maximum diameter of approximately 6 nm. It is therefore clear that the dendrimer analyzed here is not a compact but a fluctuating structure.

This point becomes even more evident when comparing the experimental $T(q)$ (Figure 10, squares) with the form factor of a homogeneous sphere having the radius of gyration $R_{g,\infty}$ (dashed line in Figure 10). It is seen that this model of a homogeneous sphere describes the $I_S(q)$ in the Guinier region ($qR_{g,\infty} < 1$) quite well as expected from eq 13. It fails badly, however, if $qR_{g,\infty} > 2$ and predicts a distinct minimum not being visible in the experimental data. While the present q range does not give information about the finest details of the structure, the comparison shown in Figure 10 demonstrates that the model of a compact sphere can easily be ruled out. Therefore, the dendrimer of fifth generation under scrutiny here is more akin to a polymeric structure than to a dense colloidal structure.

Conclusion

The present analysis of a dendrimer of fifth generation employing SANS including contrast variation has been presented. It clearly demonstrated that the structural analysis requires the decomposition of the measured intensity according to eq 8. Only the part of $I(q)$ which scales with the square of the contrast, namely $I_S(q)$, is related to the structural information embodied in average segment density $T(r)$. Despite the restricted q range available ($qR_{g,\infty} \leq 5$), the analysis of $I_S(q)$ has shown unambiguously that $T(r)$ has its maximum at $r = 0$. This finding is in full accord with recent theoretical studies.[5−7,9]

Acknowledgment. Financial support by the Bundesministerium für Forschung und Technologie is gratefully acknowledged.

References and Notes

(1) Newkome, G. R.; Moorefield, C. N.; Vögtle, F. *Dendritic Molecules;* VCH: Weinheim, 1996.
(2) Tomalia, D. A.; Naylor, A.; Goddard, W. A. *Angew. Chem., Int. Ed.* **1990**, *29*, 138.
(3) Issberner, J.; Moors, R.; Vögtle, F. *Angew. Chem., Int. Ed.* **1994**, *33*, 2413.
(4) de Gennes, P. G.; Hervet, H. *J. Phys. (Paris)* **1983**, *44*, L351.
(5) Lescanec, R. L.; Muthukumar, M. *Macromolecules* **1990**, *23*, 2280.
(6) Mansfield, M. L.; Klushin, L. L. *Macromolecules* **1993**, *26*, 4262.
(7) Murat, M.; Grest, G. S. *Macromolecules* **1996**, *29*, 1278.
(8) Cavallo, L.; Fraternali, F. *Chem. Eur. J.* **1998**, *4*, 927.
(9) Boris, D.; Rubinstein, M. *Macromolecules* **1996**, *29*, 7251.
(10) Welch, P.; Muthukumar, M. *Macromolecules* **1998**, *31*, 5892.
(11) Uppuluri, S.; Keinath, S. E.; Tomalia, D. A.; Dvornic, P. R. *Macromolecules* **1998**, *31*, 4498.
(12) Bauer, B. J.; Briber, R. M.; Hammounda, B.; Tomalia, D. A. *Polym. Mater. Sci. Eng.* **1992**, *66*, 704.

(13) Briber, R. M.; Bauer, B. J.; Hammounda, B.; Tomalia, D. A. *Polym. Mater. Sci. Eng.* **1992**, *67*, 430.
(14) Prosa, T. J.; Bauer, B. J.; Amis, E. J.; Tomalia, D. A.; Scherrenberg, R. *J. Polym. Sci., Part B: Polym. Phys.* **1997**, *35*, 2913.
(15) Scherrenberg, R.; Coussens, B.; van Vliet, P.; Edouard, G.; Brackman, J.; de Brabander, E.; Mortensen, K. *Macromolecules* **1998**, *31*, 456.
(16) Ramzi, A.; Scherrenberg, R.; Brackman, J.; Joosten, J.; Mortensen, K. *Macromolecules* **1998**, *31*, 1621.
(17) Feigin, L. A.; Svergun, D. I. *Structure Analysis by Small-Angle X-Ray Scattering and Neutron Scattering;* Plenum Press: New York, 1987.
(18) Higgins, J. S.; Benoit, H. C. *Polymers and Neutron Scattering*; Clarendon Press: Oxford, 1994.
(19) Hyman, A. S. *Macromolecules* **1975**, *8*, 849.
(20) Hickl, P.; Ballauff, M. *Physica A* **1997**, *235*, 238.
(21) Hickl, P.; Ballauff, M.; Jada, A. *Macromolecules* **1996**, *29*, 4006.
(22) Stuhrmann, H. B.; Kirste, R. G. *Z. Phys. Chem. (Munich)* **1967**, *56*, 334.
(23) Luzatti, V.; Tardieu, A.; Mateu, L.; Stuhrmann, H. B. *J. Mol. Biol.* **1976**, *101*, 115.
(24) Archut, A.; Vögtle, F.; De Cola, L.; Azzellini, G. C.; Balzani, V.; Ramanujan, P. S.; Berg, R. H. *Chem. Eur. J.* **1998**, *4*, 699.
(25) See e.g. in: Gosh, R. E.; Egelhaaf, S. U.; Rennie, A. R. *A Computing Guide for Small-Angle Scattering Experiments;* Institut Laue Langevin: 1998.
(26) Ragnetti, M.; Oberthür, R. C. *Colloid Polym. Sci.* **1986**, *264*, 32.
(27) Banchio, A. J.; Nägele, G.; Ferrante, A.; Klein, R. *Prog. Colloid Polym. Sci.* **1998**, *110*, 54.
(28) Hummelen, J. C.; van Dongen, J. L. J.; Meijer, E. W. *Chem. Eur. J.* **1997**, *3*, 1489.
(29) Dingenouts, N.; Bolze, J.; Pötschke, D.; Ballauff, M. *Adv. Polym. Sci.* **1999**, *144*, 1.

MA982027X